1 **A novel localization based biosensor, SEDAR, visualizes spatio-temporal dynamics of**

2 **activated Ras in endogenous *Drosophila* tissues**

3 **Rishita Changede** [1,2,*]

4

5 [1]Institute of Molecular and Cell Biology, Agency for Science Technology and Research;

6 Singapore, 61 Biopolis Drive, Proteos, Singapore - 138673

7 [2]Mechanobiology Institute, National University of Singapore, 10-01 T Labs, Singapore, 117411

8 [*]Correspondence – rishitac@nus.edu.sg, Phone: +6583572479

9 Keyword: Biosensor, Receptor Tyrosine Kinase, Growth Factor Receptor, Chemotaxis,

10 Drosophila

11 Running Title: Biosensor SEDAR detects activated Ras in invivo tissues

12 **Abstract**

13 Chemokine signaling via growth factor receptor tyrosine kinases (RTKs) regulates

14 development, differentiation, growth and disease implying that it is involved in a myriad of

15 cellular processes. A single RTK, for example the Epidermal Growth Factor Receptor (EGFR),

16 is used repeatedly for a multitude of developmental programs. Quantitative differences in

17 magnitude and duration of RTK signaling can bring about different signaling outcomes.

18 Understanding this complex RTK signals requires real time visualization of the signal. To

19 visualize spatio-temporal signaling dynamics, a biosensor called SEnsitive Detection of

20 Activated Ras (SEDAR) was developed. It is a localization-based sensor that binds to activated

21 Ras directly downstream of the endogenous activated RTKs. This binding was reversible and

22 SEDAR expression did not cause any detectable perturbation of the endogenous signal. Using

23 SEDAR, endogenous guidance signaling was visualized during RTK mediated chemotaxis of

24 border cells in *Drosophila* ovary. SEDAR localized to both the leading and rear end of the

25 cluster but polarized at the leading edge of the cluster. Perturbation of RTKs that led to delays

26 in forward migration of the cluster correlated with loss of SEDAR polarization in the cluster.

27 Gliding or tumbling behavior of border cells was a directly related to the high or low

28 magnitude of SEDAR polarization respectively, in the leading cell showing that signal

29 polarization at the plasma membrane provided information for the migratory behavior.

30 Further, SEDAR localization to the plasma membrane detected EGFR mediated signaling in

31 five distinct developmental contexts. Hence SEDAR, a novel biosensor could be used as a

32 valuable tool to study the dynamics of endogenous Ras activation in real time downstream of

33 RTKs, in three-dimensional tissues, at an unprecedented spatial and temporal resolution.

34

35 **Significance**

36 Chemokine signaling is vital for many cellular processes. It is thought that the strength and

37 duration of the RTK signaling can regulate different downstream outcomes in invivo tissues.

38 A biosensor is needed to visualize these quantitative differences. SEDAR, a biosensor was

39 developed to visualize Ras activation immediately downstream of the RTKs. This sensor

40 visualized activation of endogenous receptors in real time, and subcellular spatial resolution.

41   SEDAR visualized signaling in several tissues, in Drosophila and can be used to understand

42   signaling in various contexts.

43

Introduction

44

45   Growth factor receptor tyrosine kinases (RTKs) are chemokine receptors that signal during

46   key developmental processes (1-3) and chemotaxis (4). Growth factor receptor such as EGFR

47   are often mutated in several cancers and are indicators of poor prognosis (5). The myriad of

48   outcomes of EGFR are brought about by few intracellular signaling pathways (6, 7). One way

49   to bring about different signaling outcomes is to regulate the magnitude i.e. strength and

50   duration of RTK activation (8, 9). Hence, visualization of endogenous RTKs signaling in real

51   time and at subcellular resolution could provide critical insights into the diverse outcomes

52   downstream of RTKs.

53   Forster Resonance Energy Transfer (FRET) based biosensors such as Raichu, reported that

54   dynamics of Ras downstream of growth factor receptor signaling (10, 11). However FRET

55   probes are not used *in vivo* to visualize dynamics of endogenous RTK signaling due to poor

56   technical challenges such as poor FRET efficiency deep within the tissue (12) and dominant

57   negative effects of high expressing FRET constructs that disrupt very subtle endogenous RTK

58   signals (13-15). RTK signaling is typically visualized *in vivo* using reporter constructs expressing

59   GFP/LacZ or phospho specific antibodies to downstream components such as Erk are suitable

60   to provide binary information of RTK activation (3, 16). To date, following the dynamics of this

61   activation in real time, that are instructive for the cell, is not possible (8). Direct visualization

62   of *in vivo* RTK signals pose problems in that, they are very subtle and antibodies to

63   phosphoPVR could not detect the subtle activation of PVR without amplification by

64   overexpressing PVR (15)*.* Recent approaches use phase separation based *in vivo* assays to

65   visualize dynamics of Erk signaling (17) which is several steps downstream of the RTK signaling

66   cascade and does not provide information on RTK activation dynamics. Mass spectrometry

67   based assay of phosphorylation events downstream of EGFR activation were visualized at

68   seconds' time scale (18), yet these may be challenging experiments to perform *in vivo*. Hence

69   a biosensor to visualize endogenous RTK activation dynamics at subcellular resolution is much

70   needed.

71   An effective biosensor to sense endogenous signals would need very low transgene

72   expression, both to detect subtle signals and to avoid interference with endogenous signaling

73   while maintaining high sensitivity towards the signal. This paper reports the development of

74   a novel localization based biosensor probe, SEnsitive Detection of Activated Ras (SEDAR), to

4

75   visualize the spatio-temporal dynamics of endogenous RTK signals in *in vivo*. Activation of Ras,

76   a small GTPase downstream of RTKs (19) and upstream of multiple signaling pathways (20)

77   was visualized by binding of highly fluorescent Ras binding domain of Raf to it (See Figure 1).

78   SEDAR visualized signaling dynamics in RTK guided (PVR and EGFR) chemotactic border cell

79   migration that occurs during *Drosophila* oogenesis (16, 21, 22). Border cells are a group of 6-

80   8 cells that delaminate from the follicular epithelium and migrate through the germline

81   towards the developing oocyte (23, 24). SEDAR polarized at the leading edge of the cluster

82   and the magnitude of this polarization determined the size of protrusions. In addition to

83   border cells, SEDAR detected the subcellular localization of activated Ras immediately

84   downstream of EGFR signaling in several tissues during *Drosophila* development (1, 3). Hence

85   SEDAR can have wide spectrum of applications in understanding the complex regulation of

86   varied signals mediated by Ras activation. Taken together, SEDAR is a novel biosensor that

87   visualized spatio-temporal dynamics of Ras activation in *in vivo* tissues.

88

89   **Results**

90   **Design and validation of the biosensor**

91   Ras, a GTPase activated downstream of several RTKs (for example, PVR, EGFR, (16, 25-27) was

92   visualized by specific recruitment of Ras binding domain (RBD) of Raf, a MAPKKK, to GTP

93   bound activated Ras (Figure S1a). Different combinations of minimal or extended RBD were

94   fused to a linear string of ten molecules of GFP (Figure S1b). Combined fluorescence of ten

95   GFP molecules increased the sensitivity of visualization of the RTK signal and allowed for low

96   expression of the transgene. For ubiquitous expression, a gentle and acute induction of a

97   heat-shock promoter (hs) was used (see methods). Expression under a UAS promoter gave

98   rise to high expression, inadequate to detect low signals.

99   To identify the most suited biosensor design, localization of all hs-sensors were observed in a

100   well-documented example of RTK signaling in the *Drosophila* ovary, namely EGFR signaling in

101   response to the dorsal ventral graded distribution of Gurken ligand secreted by *Drosophila*

102   oocyte. Dorsal follicular epithelium activated EGFR signaling whereas non signaling ventral

103   cells serve as a negative control (28, 29) (Figure 1a, 1b). The signal was quantified as intensity

104   of GFP at the apical plasma membrane of follicle cells normalized to the cytoplasmic intensity

105   of GFP (Figure 1a, 1b). Several Ras biosensors did not localize specifically to the plasma of the

106   dorsal follicular epithelium (Figure S1b, S1c). Two of the five RAS biosensors (HS-RBD-10XGFP

107   and HS-2RBD-10xGFP) were preferentially recruited to the apical plasma membrane in the

108   dorsal cells, with no detectable recruitment in ventral cells (Figure 1b, S1b, S1c). Sensitivity of

109   2RBD-10xGFP was higher than RBD-10XGFP (Figure S2a) and was chosen for further

110   experiments and it was called SEDAR.

111   To validate SEDAR as a sensor for activated RTKs, we tested SEDAR localization in border cell

112   clusters overexpressing PVR. Janssens et al, showed preferential enrichment of phosphoPVR

113   to the front of these clusters. SEDAR enrichment was distinctly visible in epithelium where

114   apical plasma membrane had very regular boundaries, however such distinct enrichment was

115   not immediately visible in border cell clusters. To measure subcellular localization of SEDAR

116   in border clusters over expressing PVR, a region of interest were marked by line 0.4μm thick

117   and 1-3μm long at the front edge(f) and side edge(s) of the same cell in image of the

118   membrane dye and the average intensity measured in the SEDAR image (Figure S2a). SEDAR

119   mimicked phosphoPVR localization and showed a preferential enrichment at the front

120   compared to the side of the leading cell in the border cell cluster (Figure 1e, n=166 clusters,

121   Figure S2a) suggesting that SEDAR could sense RTK signaling.

122

A ratiometric method for robust detection of SEDAR in cells with irregular membrane

124   Membrane label marked the plasma membrane of the border cell cluster and the nurse cells,

125   introducing errors in the measurements hence neutral cytoplasmic marker, slbo-TurboRFP,

126   was co-expressed to demarcate the border cell clusters. Due to the polyploid nature of the

127   border cells, the expression pattern of SEDAR in different border cells varied (Figure S1d) so

128   mild expression of SEDAR was induced specifically in the border cells under the control of the

129   genomic region upstream of *slbo* and its 5'UTR (Figure 1d). A ratio of SEDAR image to the

130   cytoplasmic RFP image (Figure 1e, Ratio) showed preferential SEDAR enrichment at the front

131   of the border cell cluster (Figure 1e, last panel), making it well suited to measure plasma

132   membrane recruitment of SEDAR in cells with irregular boundaries.

133   To measure subcellular localization of SEDAR, ROIs were marked in the RFP image, at the front

134   (f) and side (s) of the leading cell, and measured in the Ratio image (Figure 1e). All

6

135   measurements were normalized to cytoplasm (box'c', Figure 1e), marked to carefully avoid

136   the nucleus Figure1d). This parameter was termed localization index (f/c). Value of 1 or less

137   corresponded to no enrichment of SEDAR at the plasma membrane, greater than 1 indicated

138   recruitment of SEDAR at the plasma membrane. To test if this was a general enrichment of

139   SEDAR at the entire plasma membrane or a specific enrichment at the front edge of the

140   leading cell, the signal at the front edge and side were compared (f/s). This was termed as the

141   polarization index. Wild type clusters had a high localization (2.84±0.59, Mean±SD, Figure 1e,

142   1f - control) and polarization index (1.59±0.57, Figure 1e, 1h-control). phosphoPVR antibody

143   could only detect signal upon PVR overexpression and was not sensitive enough to report the

144   subtle endogenous signal. This is the first observation of the endogenous RTK signaling.

145   Migration speed of the border cell clusters is sensitive to perturbation of RTK signal (26).

146   Expressing of SEDAR did not perturb this migration speed (Figure S2b) showing that low levels

147   of endogenous guidance signal could be monitored in cells with irregular and dynamically

148   changing cells without disrupting it.

149

150   **SEDAR localization was stringently dependent upon RTK and Ras activation**

151   To test the specificity of SEDAR signal to guidance input provided by PVR and EGFR, both

152   receptors were simultaneously knocked down using RNAi (Figure 1f, (30). Expression of RNAi

153   disrupted SEDAR recruitment to the plasma membrane (Figure S2c). SEDAR localization index

154   was reduced below 1. As there was no preferential recruitment at the plasma membrane, if

155   the measurement method is accurate the polarization index should also be below 1. It was

156   measured to be 0.93 (±0.27). This result confirmed that SEDAR localization at the leading edge

157   of border cell cluster stringently depended on guidance signal provided by the RTKs. Thus,

158   SEDAR specifically detected subcellular signaling from endogenous guidance receptors during

159   invasive cell migration.

160   To validate that SEDAR detected signaling by Ras, two distinct RNAi construct targeting the

161   major Ras, Ras85D, were expressed individually with SEDAR. SEDAR intensity at the

162   membrane was not visible in RNAi expressing border cell clusters (Figure S2c). Ras RNAi

163   expression decreased localization index to 1.66 (±0.5) in GD line and 1.37 (±0.51) in TRiP line

164   (Figure 1g), possible due to incomplete knockdown of Ras. The polarization index was 1.17

7

165 (±0.35) and 1.22(±0.41) respectively in the two RNAi lines (Figure 1h). In contrast, expression

166 of RasV12, a constitutively activated form of Ras, showed an enrichment of SEDAR at the

167 entire plasma membrane of all border cells (Figure S2e). Together, it showed that SEDAR

168 localization at the leading edge specifically reported activation of Ras.

169

170 **SEDAR visualized dynamics of RTK signaling during border cell migration**

171 We next assayed SEDAR localization in real time. It showed a front localization compared to

172 the side of the same cell (Figure 2a, 2b). Average signal over the entire outer membrane of

173 the border cell cluster was much lower and the bias was averaged out, serving as a control

174 (Figure 2b). SEDAR localization at the leading edge of the cluster showed a cyclic pattern of

175 increasing and decreasing signal, which was not observed at the side of the cell (Figure 2a, 2b,

176 Video S1), similar to that observed in migratory cells in tissue culture (31).

177 We assayed whether border cell behavior was directed by spatial activation of RTK within the

178 border cell clusters. Border cell migration was divided into early phase, until the border cells

179 reach 50% distance during the posterior migration and the late phase from 50% until they

180 reach the oocyte (30). Early migration is characterized by persistent gliding movement with a

181 dominant leader cell that has large protrusions whereas the late phase of migration is

182 characterized by tumbling behavior where leader cells are frequently exchanged and have

183 short lived, small protrusions. Strong front bias was observed in the leading cell of early

184 migratory clusters (Figure 2d). Front bias was also observed in late migratory cluster (Figure

185 2c, 2e)

186 Localization and polarization index of SEDAR were measured in the lead and the rear cell. For

187 the rear cell, these parameters were measured at the back of the rear cell ('r' Figure S3a)

188 compared to its cytoplasm or side of the same cell. Polarization index of front cell over the

189 rear cell measured the cell extrinsic cluster polarity of RTK activation.

190 In wild type early migratory clusters, the leading cell showed a higher localization index (2.2

191 ±0.81, Figure 2f) compared to the rear cell (1.89±0.6, Figure 2f) suggesting an overall front

192 bias of SEDAR localization in the migrating border cell cluster. In the front cell, polarization

193 index was higher (1.75±0.96, Figure 2g) compared to the rear cell (1.37±1.07, Figure 2g). Cell

8

194   extrinsic cluster polarization was 28.5 percent higher at the front compared to the back of the

195   entire cluster. In late migratory clusters, the localization index was 2.02 (±0.7) in the lead cell

196   and 1.54 (±0.47) in the rear cell (Figure 2f). It is reduced compared to the early clusters but

197   there is signal. The polarization index was reduced to 1.33 (±0.47) in the lead cell and 1.04

198   (±0.29) in the rear cell (Figure 2g). The magnitude of the cell intrinsic polarity in the lead cell

199   was reduced yet the cell extrinsic cluster polarity was maintained at 27.9 percent higher in

200   the front of the cluster compared the back of the cluster. This indicated that cell extrinsic

201   cluster polarity dictated forward migration and magnitude of cell intrinsic polarity could

202   dictate the mode of migration i.e. gliding or tumbling. Low magnitude of outward polarization

203   in the rear cell correlated with fewer protrusions observed in the rear cell (30). SEDAR was

204   assayed upon RTK perturbation which mimicked specific aspects of directed migration or

205   migratory behavior

206

207   **Spatial localization of RTK activation determined behavior and migration of border cells**

208   RTK perturbation disrupted directed migration or (overexpression) mimicked specific aspects

209   of early or late migratory behavior. For these analyses, early migratory clusters were imaged.

210   This allowed for comparison of clusters at the similar stage of migration cells as PVR^{DN}EGFR^{DN}

211   and EGFR overexpressing clusters were delayed during migration (30).

212   To test if intracellular polarization index of SEDAR correlated with directed migration, SEDAR

213   localization was assayed in border cells clusters where directed migration of the cluster was

214   disrupted by simultaneous overexpression of the dominant negative RTKs (RTK^{DN}-

215   EGFR^{DN}PVR^{DN}) without affecting the motility of the individual cells (30). Over time, no

216   preferential front localization of SEDAR was observed at the front of the leading cell (Figure

217   3a, 3b). Though SEDAR localized to the plasma membrane (Figure 3c, Table S1). It was diffused

218   as observed by the polarization index value of ~1 (lead cell – 1.16±0.44, rear cell-1.2±0.43,

219   Figure 3d, Table S1) indicating loss of cell intrinsic polarity. The cell extrinsic polarization of

220   the border cell cluster was lost with a marginal increase in the rear cell (3.2 percent) compared

221   to the lead cell. This could explain the loss of directed migration observed within these

222   clusters (30). SEDAR localization showed that cell extrinsic polarization of RTK signal in the

223   border cell cluster guided migration of it. Further, no persistent protrusion was observed in

224   the lead cell correlating with low magnitude of RTK polarization in the lead cell.

225   PVR overexpression promoted efficient gliding movement typical of the early phase of

226   migration (26, 30). In border cell clusters overexpressing PVR (Figure 3e), the polarization

227   index of SEDAR in the lead cell is increased to 1.82 (±0.79, Figure 3h), yet the amount of signal

228   within the leading cell is comparable to wild type (localization index lead cell – 2.15±0.83, rear

229   cell – 2.01±0.66, Figure 3g, Table S1). This correlated well with the persistent leader cell and

230   large strong protrusions. In the rear cell, SEDAR localization is outward polarized 1.26 (±0.44)

231   but reduced slightly compared to the wild type clusters (Figure 3h). The cell extrinsic cluster

232   polarity is increased to 44.6 percent compared to the 28.3 percent in the wild type. This

233   correlated well with persistent forward migration of the border cell cluster.

234   EGFR overexpression operated primarily via tumbling mode of migration where a persistent

235   leader cell was absent (26, 30). In border cell clusters overexpressing EGFR (Figure 3f), SEDAR

236   showed comparable localization index (lead cell- 2.33±0.8, rear cell 1.88±0.58, Figure 3g).

237   However, the polarization index of the lead cell was reduced to 1.37 (±0.57, Figure 3h)

238   comparable to the late phase of migration. Next, the rear cell also showed an outward

239   polarization of 1.26 (±0.39, Figure 3h) which reduced the cell extrinsic cluster polarity to a

240   mere 8.3 percent; over five-fold lower than that observed within the clusters overexpressing

241   PVR and three-fold lower than wild type early clusters. Loss of cell extrinsic cluster polarity

242   correlated with severe delays in migration of the border cell clusters as overserved with EGFR

243   overexpression (reported earlier, (30), suggesting that it determined forward movement of

244   the cluster. Hence, SEDAR localization patterns detected activation of both PVR and EGFR.

245   Low magnitude of cell intrinsic polarity of SEDAR recruitment in lead cell of late migratory

246   cluster, rear cells of early and late migratory cluster, and lead cell of EGFR[DN]PVR[DN] and EGFR

247   overexpression explained the observed absence of large protrusions in each of these cluster

248   (30) whereas large protrusions observed in lead cell of early migratory cluster and PVR

249   overexpression correlated with large protrusions and gliding motility (30). Next, high cell

250   extrinsic cluster polarity determined effective forward migration without delays as observed

251   in PVR overexpression, WT early and late migratory clusters and reduction in this polarity led

252   to severe delays as observed in PVR[DN]EGFR[DN] and EGFR overexpression (30). Taken together,

10

253   these results showed that differential spatial activation of RTK signaling at the plasma
254   membrane could directly alter behavior and migration of border cells.

255

256   **SEDAR localized to plasma membrane downstream of EGFR or PVR signaling in different**
257   **tissues in *Drosophila*.**

258   Could SEDAR sense RTK activation in different tissues? EGFR signaling is key for many events
259   during development. SEDAR localization was assayed in tissues which use EGFR signaling
260   during development.

261   During *Drosophila* embryogenesis, EGFR function is required in the epidermis for proper
262   dorsal closure and its activity is observed by phosphoErk (32). SEDAR was recruited to the
263   plasma membrane of the epidermis during dorsal closure (Figure 4a). Stage 16 embryos
264   served as negative control, where no EGFR signaling is reported in the epidermis. In these
265   embryos, SEDAR appeared diffused in the cytoplasm and no preferential localization was
266   observed at the plasma membrane (Figure S4).

267   During early stages of *Drosophila* oogenesis, Erk is activated in the follicular epithelium.
268   SEDAR localized to the apical plasma membrane of the follicular epithelium in stage 2-7
269   (Figure 4b). In stage 8, ERK is activated downstream of EGFR in the posterior follicle cells (33).
270   In these cells, SEDAR is localized to the apical plasma membrane of the dorsal follicle cells
271   (Figure 4b).

272   Overexpression of PVR in the ovariole, under *slboGal4*, leads to high level of PVR expression
273   in few cells of the follicular epithelium, some which in turn activated downstream signals
274   (Figure 4c (15)). In cells overexpressing PVR labeled with total PVR antibody (marked with
275   arrow, Figure 4c (15), SEDAR localized to the plasma membrane whereas no preferential
276   localization was observed in cells not activating PVR within the same tissues (Figure 4c).
277   Similarly, in cells overexpressing EGFR (as observed in EGFR antibody staining, Figure 4c),
278   SEDAR localized to the plasma membrane, whereas diffuse cytoplasmic localization of SEDAR
279   was observed in the neighboring cells not overexpressing EGFR (Figure 4c).

11

280   Taken together, this paper demonstrated in 5 different *Drosophila* tissues that SEDAR could

281   detect endogenous activated Ras, particularly downstream of EGFR or PVR at subcellular

282   resolution. Its localization could be monitored in real time in endogenous tissues.

283

284   **Discussion**

285   Real-time biosensors that reflect activity of key signaling molecules in the cell have greatly

286   expanded the possibilities for quantitative molecular analysis of dynamic processes such as

287   cell migration but they are limited to analyses in 2D cell culture systems. Observing signaling

288   events in physiological conditions was much needed. In this paper, an approach to study

289   signaling via the small GTPase Ras using highly fluorescent recruitment-based probes in cells

290   is presented. Biosensor, SEDAR, specifically detected Ras activation downstream of growth

291   factor receptors in multiple instances in *Drosophila* epithelial tissue. In cells with irregular

292   membranes such as migrating border cells, SEDAR detected endogenous signaling without

293   any amplification of the signal (overexpression of PVR) indicating that it is more sensitive than

294   antibodies to phosphorylated receptors (15). SEDAR allowed detection of RTK activation *in*

295   *vivo* in real time.

296   SEDAR detected signal downstream of the chemotactic RTKs. This detection of endogenous

297   signal provided an evidence of how RTKs could regulate distinct behaviors observed in the

298   clusters. Comparing wild type and guidance-defective clusters, showed that guidance

299   signaling is indeed reflected by SEDAR and detectable by the method presented here.

300   Magnitude of cell intrinsic polarity determined the behavior of the leading cell indicating that

301   the magnitude of subcellular RTK activation was informative to the cell. A higher magnitude

302   of RTK activation at the leading edge could be above the threshold required for Rac activation,

303   which is crucial for cell migration and in turn could promote lamellipodia like large protrusion

304   formation (34-37). Rac is directly downstream of PDGF (38). PVR (PDGF VEGF like receptor)

305   has a high magnitude of cell intrinsic front polarity of SEDAR and Rac activation is high in the

306   leading cell (34, 39). Together this suggests that high magnitude of RTK activation, primarily

307   downstream of PVR can promote formation of large protrusions in the leading edge via Rac.

308   EGFR stimulated small protrusions and it was shown to directly interact with Cdc42 that

309   promotes filopodia like protrusions (40).

310   Cell extrinsic cluster polarity was informative to guide the forward directed migration of the

311   border cell cluster. It provides a direct evidence for strong local activation and mild global

312   inhibition of RTK signaling (41-44). Single cells that do not have RTK signaling could not occupy

313   the position of the leading cell (45) implying a necessity of high signal in the leading cell.

314   Secondly, cell extrinsic cluster polarity provided an explanation for the polarization of two

315   crucial downstream signals within the cluster i.e. tension in E-cadherin and Rac activation in

316   the front of the border cells cluster (34, 46). Previous evidences fell short of explaining these

317   critical signal gradients essential for migration wherein gradient of Pvf1 in the egg chamber

318   has been difficult to detect and there is no difference in the amount of E-cadherin in the front

319   and back of the cluster. To confirm these results, expression of RTK^{DN} led to loss of cell

320   extrinsic cluster polarity and both its features were absent viz, forward migration was severely

321   delayed and it corresponded to similar loss of polarization of tension in E-cadherin (46).

322   Further, cell extrinsic cluster polarity in the direction of migration provided evidence that

323   there is a long-range signal integration of the RTKs over the length scale of the cluster (44). E-

324   cadherin and Rab 11 could mediate long-range communication between border cells along

325   the length of the cluster primarily via cell-cell contacts (46, 47).

326   In general, the strategy of low-level expression of highly fluorescent recruitment sensors

327   coupled with normalization is useful for many spatially organized signaling events in tissues.

328   Given that the signals probed by the sensors are used repeated in several tissues to bring

329   about a myriad of functions, they could be adapted to any tissue of choice. Most epithelial

330   tissues are very well suited for analyses as they have straight well-defined apical membrane,

331   allowing for easy detection of the signal. With the ratiometric approach, it can be adapted to

332   cells with irregular plasma membrane. Expression under the heat shock promoter can restrict

333   the expression of the sensor temporally thereby allowing for precise analyses at a

334   developmental time of choice. The versatility and universality of the localization based sensor,

335   SEDAR, has a potential to provide many insights into the signaling dynamics of various

336   different RTKs upstream of Ras. Sensors based on designs similar to SEDAR could be adapted

337   to other signaling pathways to visualize them in three-dimensional *in vivo* tissues.

338

339

340 **Acknowledgements**

346

347 **Conflict of interest**

348 The author declares no conflict of interest.

349

350 **Materials and Methods:**

351 SEDAR is freely available upon request from the author.

352 *Molecular cloning:*

353 For Ras-sensor tests, short or extended Ras-binding domains from Drosophila Raf/polehole

354 coding sequence (supplemental Figure S1) were cloned into pmEGFP10N-1 (kind gift from Jan

355 Ellenberg, EMBL). This was cloned into pCasper-HS and finally into pAttB, transgenic flies

356 made by P-element transformation. For border cell, RAS-sensor, 2 copies of extended RAS

357 binding domains of Drosophila Raf (amino acids 120-307) separated by a 6-glycine linker, were

358 cloned into, and then to pAttB-slbo3.6. pAttB-slbo3.6 was made by inserting a 3.6 kb genomic

359 fragment from upstream of the slbo coding region (including part of the border cell enhancer

360 (Rørth et al 1998) and a long 5' UTR with several ultra-short ORFs. Primers: Forward-

361 GAAGTGATGCTAGCGGATCCAGCTGCGGCGTTTTATTCTCACGCT and Reverse-

362 CGCAGATCTGTTAACGAATTCTGCAGATTGTTTAGC and poly-adenylation sequences from SV40

363 into pAttB. Transgenes were insertion into flies with AttP at 86Fb. For 2xslbo-turboRFP,

364 turboRFP [Invitrogen] was sub-cloned downstream of two copies of the slbo enhancer (Rørth

365 1998) and a minimal promoter for high expression in anterior follicle cells starting at stage 6,

366 transferred to pCasper-AttB and inserted at the VK33 AttP site. AttP flies were obtained from

367 Bloomington.

368

Flies and genetics:

Fly stocks were obtained from the Bloomington and Vienna Drosophila stock centers. RNAi lines used were GD13502 for *Pvr*, GD43268 for *Egfr* (see Poukkula et al), GD12553 and TRiPGL00336 for *Ras85D*. All UAS-RNAi constructs were expressed under control of actin-flipout-Gal4 (AFG) control, driving robust expression in all somatic cells after heat shock–induced expression (37^0C 30 minutes) of FLP recombinase two days prior to dissection and imaging. PVR^{DN}, EGFR^{DN}, UAS-PVR, UAS-EGFR (see Duckek, Duckek et al) were expressed under slbo-GAL4 control, which drives expression in outer (non-polar) border cells.

For imaging, 2-3 day old females resulting from an outcross, maintained at 25^0C, and incubated about 20 hours with wet yeast were used. All in w^{1118} mutant background. HS-sensor expression was induced by heat shock at 34^oC for 20 minutes and flies were allowed to recover at room temperature for 3 hours prior to imaging.

Egg chamber dissection and imaging:

Ovaries and egg chambers were dissected in dissection medium (Schneider's medium [Gibco] +5 µg/ml insulin [Sigma]) and stage 9 egg chambers transferred to imaging medium (dissection medium + 2.5% fetal calf serum [Hyclone] + 2 mg/ml trehalose [Fluka] +5 µM methoprene [Sigma] + 1 µg/ml 20-hydroxyecdysone [Sigma] + 50 ng/ml adenosine deaminase [Roche] in poly-lysine-coated imaging chambers [Nunc] at room temperature. Videos were recorded by an inverted confocal microscope [SP5; Leica] with a 63×, 1.2 NA Plan Apochromat water immersion objective, 4x zoom and 2 times line average. The time interval between images was 10 seconds. Egg chambers were aligned by rotating the scan field with the anterior tip of the egg chamber aligned to the left and the image x axis going from this point through the middle of the oocyte (far right). The focal plane with border cells having the furthest front tip was chosen for imaging. After imaging (10 minutes) different focal planes were rechecked to ensure the right focal plane had been used in the whole video. Egg chambers or videos with defects were discarded.

395

396

397   *Image analysis*:

398   To generate ratiometric images, GFP and RFP images were first smoothed by Gaussian Blur

399   (sigma 1.0) and then the GFP image was divided by the RFP image (Image J). The front, side

400   and back signals were measured in 1.5µm long and 0.4 µm width lines in ratio-metric images

401   and cytoplasmic signal as a small square box inside the front cell. For each video, 30 to 60

402   images were measured as long as the leading cell edge or rear cell edge that was being

403   measured was in the optical plane being imaged.

404   *Immunostaining:*

405   After dissection ovaries were fixed in 4% paraformaldehyde for 20 min. Ovaries were washed

406   in buffer [50 mM Tris-HCl (pH 7.4), 150 mM NaCl, 0.05%, 1 mg/mL BSA] for 30 minutes at RT

407   and manually dissociated into single egg chambers by pipetting them using 200ml tip. They

408   were blocked in 5 mg/mL BSA for 30 minutes and incubated overnight at 4 °C with primary

409   antibody 1:200 (16) for total PVR or total EGFR) and subsequently incubated with

410   fluorescently labelled secondary antibody 1:200 (Jackson Immunoresearch Laboratories)+

411   rhodamine-coupled phalloidin (Molecular Probes).

412

413   **References**

414   1.   Shilo BZ (2003) Signaling by the Drosophila epidermal growth factor receptor pathway

415   during development. *Exp Cell Res* 284(1):140-149.

416   2.   Sopko R & Perrimon N (2013) Receptor tyrosine kinases in Drosophila development. *Cold*

417   *Spring Harb Perspect Biol* 5(6).

418   3.   Gabay L, Seger R, & Shilo BZ (1997) In situ activation pattern of Drosophila EGF receptor

419   pathway during development. *Science* 277(5329):1103-1106.

420   4.   Friedl P & Gilmour D (2009) Collective cell migration in morphogenesis, regeneration and

421   cancer. *Nat Rev Mol Cell Biol* 10(7):445-457.

422   5.   Nicholson RI, Gee JM, & Harper ME (2001) EGFR and cancer prognosis. *Eur J Cancer* 37 Suppl

423   4:S9-15.

424   6.   Lemmon MA & Schlessinger J (2010) Cell signaling by receptor tyrosine kinases. *Cell*

425   141(7):1117-1134.

426   7.   Lusk JB, Lam VY, & Tolwinski NS (2017) Epidermal Growth Factor Pathway Signaling in

427   Drosophila Embryogenesis: Tools for Understanding Cancer. *Cancers (Basel)* 9(2).

428 8. Zinkle A & Mohammadi M (2018) A threshold model for receptor tyrosine kinase signaling
429   specificity and cell fate determination. *F1000Res* 7.

430 9. Marshall CJ (1995) Specificity of receptor tyrosine kinase signaling: transient versus
431   sustained extracellular signal-regulated kinase activation. *Cell* 80(2):179-185.

432 10. Nakamura T, Kurokawa K, Kiyokawa E, & Matsuda M (2006) Analysis of the spatiotemporal
433   activation of rho GTPases using Raichu probes. *Methods Enzymol* 406:315-332.

434 11. Mochizuki N*, et al.* (2001) Spatio-temporal images of growth-factor-induced activation of Ras
435   and Rap1. *Nature* 411(6841):1065-1068.

436 12. Eder D, Basler K, & Aegerter CM (2017) Challenging FRET-based E-Cadherin force
437   measurements in Drosophila. *Sci Rep* 7(1):13692.

438 13. Jekely G, Sung HH, Luque CM, & Rorth P (2005) Regulators of endocytosis maintain localized
439   receptor tyrosine kinase signaling in guided migration. *Dev Cell* 9(2):197-207.

440 14. Assaker G, Ramel D, Wculek SK, Gonzalez-Gaitan M, & Emery G (2010) Spatial restriction of
441   receptor tyrosine kinase activity through a polarized endocytic cycle controls border cell
442   migration. *Proc Natl Acad Sci U S A* 107(52):22558-22563.

443 15. Janssens K, Sung HH, & Rorth P (2010) Direct detection of guidance receptor activity during
444   border cell migration. *Proc Natl Acad Sci U S A* 107(16):7323-7328.

445 16. Duchek P, Somogyi K, Jekely G, Beccari S, & Rorth P (2001) Guidance of cell migration by the
446   Drosophila PDGF/VEGF receptor. *Cell* 107(1):17-26.

447 17. Zhang Q*, et al.* (2018) Visualizing Dynamics of Cell Signaling In Vivo with a Phase Separation-
448   Based Kinase Reporter. *Mol Cell* 69(2):347.

449 18. Reddy RJ*, et al.* (2016) Early signaling dynamics of the epidermal growth factor receptor.
450   *Proc Natl Acad Sci U S A* 113(11):3114-3119.

451 19. Margolis B & Skolnik EY (1994) Activation of Ras by receptor tyrosine kinases. *J Am Soc
452   Nephrol* 5(6):1288-1299.

453 20. Tan PB & Kim SK (1999) Signaling specificity: the RTK/RAS/MAP kinase pathway in
454   metazoans. *Trends Genet* 15(4):145-149.

455 21. Duchek P & Rorth P (2001) Guidance of cell migration by EGF receptor signaling during
456   Drosophila oogenesis. *Science* 291(5501):131-133.

457 22. Lee T, Feig L, & Montell DJ (1996) Two distinct roles for Ras in a developmentally regulated
458   cell migration. *Development* 122(2):409-418.

459 23. Montell DJ (2003) Border-cell migration: the race is on. *Nat Rev Mol Cell Biol* 4(1):13-24.

460 24. Prasad M & Montell DJ (2007) Cellular and molecular mechanisms of border cell migration
461   analyzed using time-lapse live-cell imaging. *Dev Cell* 12(6):997-1005.

462   25.   Wasserman JD & Freeman M (1998) An autoregulatory cascade of EGF receptor signaling
463   patterns the Drosophila egg. *Cell* 95(3):355-364.

464   26.   Bianco A*, et al.* (2007) Two distinct modes of guidance signalling during collective migration
465   of border cells. *Nature* 448(7151):362-365.

466   27.   Sims D, Duchek P, & Baum B (2009) PDGF/VEGF signaling controls cell size in Drosophila.
467   *Genome Biol* 10(2):R20.

468   28.   Brand AH & Perrimon N (1994) Raf acts downstream of the EGF receptor to determine
469   dorsoventral polarity during Drosophila oogenesis. *Genes Dev* 8(5):629-639.

470   29.   James KE, Dorman JB, & Berg CA (2002) Mosaic analyses reveal the function of Drosophila
471   Ras in embryonic dorsoventral patterning and dorsal follicle cell morphogenesis.
472   *Development* 129(9):2209-2222.

473   30.   Poukkula M, Cliffe A, Changede R, & Rorth P (2011) Cell behaviors regulated by guidance
474   cues in collective migration of border cells. *J Cell Biol* 192(3):513-524.

475   31.   Machacek M*, et al.* (2009) Coordination of Rho GTPase activities during cell protrusion.
476   *Nature* 461(7260):99-103.

477   32.   Shen W*, et al.* (2013) Modulation of morphogenesis by Egfr during dorsal closure in
478   Drosophila. *PLoS One* 8(4):e60180.

479   33.   Cheung LS, Schupbach T, & Shvartsman SY (2011) Pattern formation by receptor tyrosine
480   kinases: analysis of the Gurken gradient in Drosophila oogenesis. *Curr Opin Genet Dev*
481   21(6):719-725.

482   34.   Wu YI*, et al.* (2009) A genetically encoded photoactivatable Rac controls the motility of living
483   cells. *Nature* 461(7260):104-108.

484   35.   Heasman SJ & Ridley AJ (2008) Mammalian Rho GTPases: new insights into their functions
485   from in vivo studies. *Nat Rev Mol Cell Biol* 9(9):690-701.

486   36.   Rottner K, Hall A, & Small JV (1999) Interplay between Rac and Rho in the control of
487   substrate contact dynamics. *Curr Biol* 9(12):640-648.

488   37.   Steffen A*, et al.* (2013) Rac function is crucial for cell migration but is not required for
489   spreading and focal adhesion formation. *J Cell Sci* 126(Pt 20):4572-4588.

490   38.   Pertz O, Hodgson L, Klemke RL, & Hahn KM (2006) Spatiotemporal dynamics of RhoA activity
491   in migrating cells. *Nature* 440(7087):1069-1072.

492   39.   Wang X, He L, Wu YI, Hahn KM, & Montell DJ (2010) Light-mediated activation reveals a key
493   role for Rac in collective guidance of cell movement in vivo. *Nat Cell Biol* 12(6):591-597.

494 40. Hirsch DS, Shen Y, & Wu WJ (2006) Growth and motility inhibition of breast cancer cells by
495   epidermal growth factor receptor degradation is correlated with inactivation of Cdc42.
496   *Cancer Res* 66(7):3523-3530.

497 41. Iglesias PA & Devreotes PN (2012) Biased excitable networks: how cells direct motion in
498   response to gradients. *Curr Opin Cell Biol* 24(2):245-253.

499 42. Levchenko A & Iglesias PA (2002) Models of eukaryotic gradient sensing: application to
500   chemotaxis of amoebae and neutrophils. *Biophys J* 82(1 Pt 1):50-63.

501 43. Ridley AJ*, et al.* (2003) Cell migration: integrating signals from front to back. *Science*
502   302(5651):1704-1709.

503 44. Meinhardt H (1999) Orientation of chemotactic cells and growth cones: models and
504   mechanisms. *J Cell Sci* 112 (Pt 17):2867-2874.

505 45. Inaki M, Vishnu S, Cliffe A, & Rorth P (2012) Effective guidance of collective migration based
506   on differences in cell states. *Proc Natl Acad Sci U S A* 109(6):2027-2032.

507 46. Cai D*, et al.* (2014) Mechanical feedback through E-cadherin promotes direction sensing
508   during collective cell migration. *Cell* 157(5):1146-1159.

509 47. Ramel D, Wang X, Laflamme C, Montell DJ, & Emery G (2013) Rab11 regulates cell-cell
510   communication during collective cell movements. *Nat Cell Biol* 15(3):317-324.

511

512

513

514 **Figure legends**

515 **Figure 1:** SEDAR visualized RTK activation downstream of Ras signaling (a) schematic
516 representation of localization of SEDAR to the apical membrane upon activation of RTK signal in
517 epithelium. (b) schematic representation of Drosophila egg chamber where the Dorsal follicular
518 epithelium cells (in proximity to the oocyte nucleus) respond to Gurken signaling from the oocyte.
519 Red box marked the region shown in SEDAR panel. SEDAR panel showed localization of SEDAR
520 in the follicular epithelium, orange circle-oocyte nucleus. Graph quantified the membrane
521 localization of SEDAR normalized to cytoplasm in the dorsal and the ventral follicle cells(n=46,
522 12 egg chambers) (c) schematic of SEDAR localization in the lead cell of the border cell cluster in
523 response to RTK signaling (d) Scatter plot of intensity at the front (f) versus the side (s) of the
524 leading cell in wild type early migrating border cell clusters, f=2s green line, f=s red line, 2f=s blue
525 line, n=166 distinct clusters, p value computed by Wilcoxon singed test (e) control:
526 *hsFLP,AFG,UAS-RFP/+; SEDAR/+*. Ratiometric image of SEDAR over cytoplasm in pseudo
527 color (LUT-fire). Box marked the zoom in region shown in the last panel. ROI measured in the
528 ration image were marked in red channel. (f & g) Box plot of localization index of the lead cell of
529 the border cell cluster in Control and RTKS RNAi (PVR and EGFR, f): *hsFLP,AFG,UAS-*
530 *RFP/hsFLP;   UAS-EGFR-RNAi/+;SEDAR/UAS-PVR-RNAi*   or   RasRNAi:
531 *hsFLP,AFG,UASRFP/hsFLP;;SEDAR/UAS-RasRNAi* (h) Box plot of Polarization index of lead
532 cell of the border cell cluster in control and RasRNAi. In all box plots, the box represented the
533 upper and lower quartile, the notch represented the median, the dot represented the mean, whiskers
534 represent standard deviation and dotted line marked equal ratio. Control n= 266, 5 movies;
535 RTKRNAi n=180, 4 movies, Ras(TRiP) RNAi n=315, 6movies, Ras (GD) RNAi n=320, 6movies.
536 ***p<0.0001, Scale 10μm.

537 **Figure 2:** SEDAR localization was polarized within the lead border cell and the border cell clusters.
538 (a) Ratiometric image sequence of SEDAR/neutral cytoplasm) of wild type early migratory cluster.
539 Pseudo color (green fire blue) represented the ratiometric image, as indicated below. Scale -10μm.
540 (b&c) Mean intensity of front (f, green), side (s, red) of the lead cell and outer membrane of the
541 entire cluster (EM, grey) over time in a migrating border cell cluster. (d&e) Scatter plot of mean
542 intensity of front(f) and side(s) membrane of the lead cell in early and late migratory cluster
543 respectively. f=2s green line, f=s red line, 2f=s blue line, p by Wilcoxon singed test (f&g) Graph
544 of localization index and polarization index of lead cell and rear cell in early migratory and late
545 migratory wild type border cell clusters. In all box plots, the box represented the upper and lower
546 quartile, the notch represented the median, the dot represented the mean, whiskers represent
547 standard deviation and dotted line marked equal ratio. In early migratory clusters, Lead cell - n=

548   1049, 20 movies; rear cell-n=710, 12 movies. Late, lead cell, n=360, 6 movies, rear cell – 240, 5

549   movies.

550

551   **Figure 3:** SEDAR polarization within the border cells correlated directed behavior of border cell

552   clusters (a, e & f) Ratiometric image sequence of SEDAR and RFP Cytoplasm of genotypes

553   indicated above the images. Scale 10μm (b) Graph showing time fluctuations of the intensity of

554   front of leading cell, side of leading cell and entire outer membrane of the border cell cluster (c &

555   g) Box plot of localization index or (d & h) polarization index in lead and rear cell of border cell

556   cluster. In all box plots, the box represented the upper and lower quartile, the notch represented the

557   median, the dot represented the mean, whiskers represent standard deviation and dotted line marked

558   equal ratio. Wild type lead- n=1049, 20 movies, rear- n=710, 12 movies; $PVR^{DN}EGFR^{DN}$ lead-

559   n=744, 13 movies, rear-n=240, 4 movies, PVR lead- n=379, 9 movies, rear-n=217, 4 movies, EGFR

560   lead- n=425, 9 movies, rear- n=420, 7movies.

561   **Figure 4:** SEDAR detected activated Ras in tissues. (a) schematic of Dorsal closure at stage 13

562   during embryogenesis, box marked the zoom in region shown in the next panel. Graph of the

563   intensity plot of line drawn in right panel (b) schematic of an ovariole showing the germ line, and

564   ovarioles until stage10. DIC image of egg chamber, scale100μm. Various stages of egg chamber

565   showing SEDAR localized to the apical membrane of follicular epithelium. Scale 10μm. Zoom in

566   of stage 7 egg chamber. (c) Follicular epithelium of stage10 egg chamber expressing slbo-Gal4 and

567   UAS PVR (top panel) or UAS DER (bottom panel) stained with anti PVR or anti DER antibody

568   (cyan), SEDAR (green) and phalloidin (red). Cell with high PVR or DER expression are marked

569   with a white arrow in each panel. Scale 10μm.
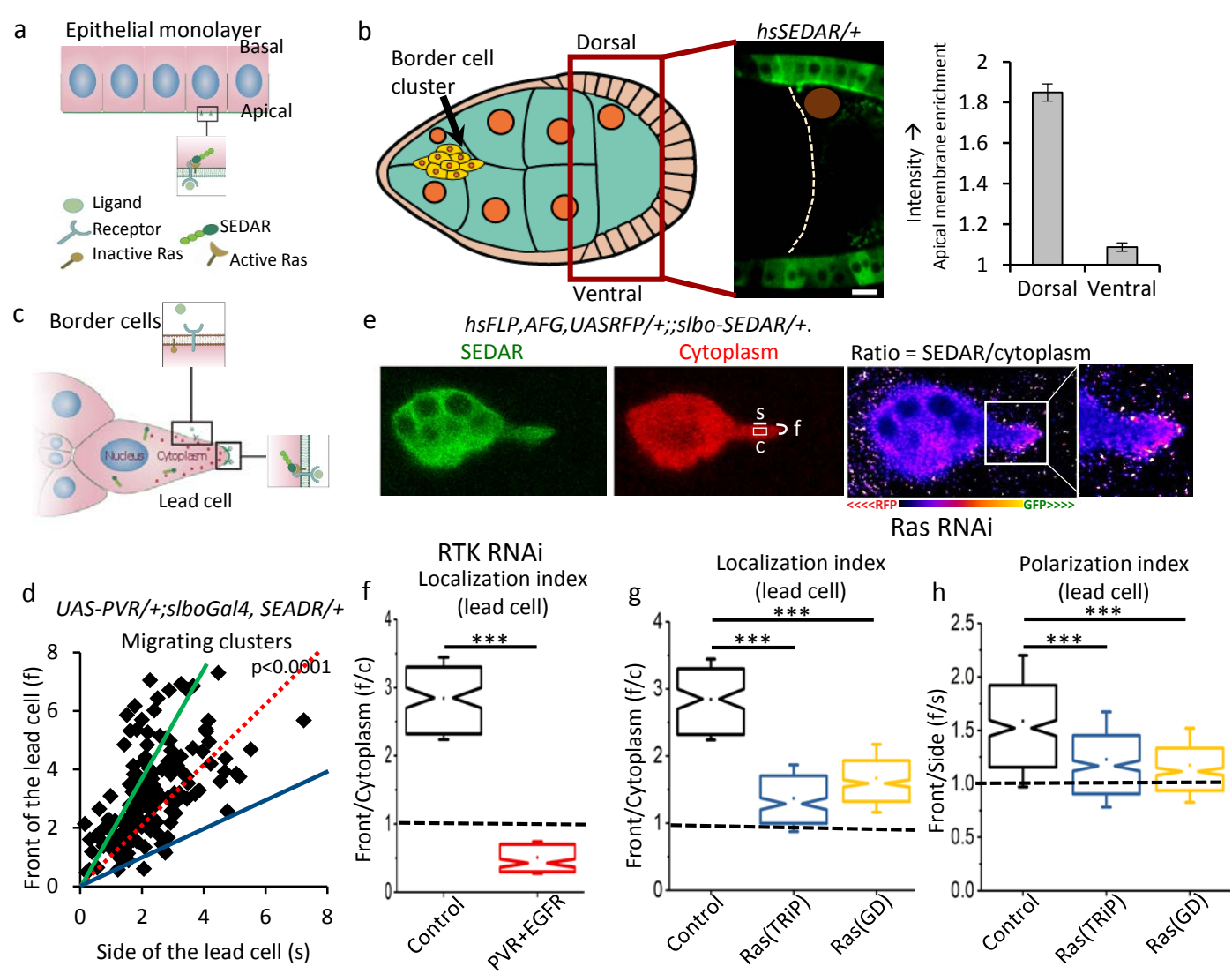
570

571

572

Figure 1

a Epithelial monolayer

Ligand
Receptor
Inactive Ras
SEDAR
Active Ras

b Border cell cluster

Dorsal

hsSEDAR/+

Ventral

Intensity →
Apical membrane enrichment

Dorsal Ventral

c Border cells

Nucleus Cytoplasm

Lead cell

e *hsFLP,AFG,UASRFP/+;;slbo-SEDAR/+.*

SEDAR   Cytoplasm   Ratio = SEDAR/cytoplasm

<<<<RFP   GFP>>>>
Ras RNAi

d *UAS-PVR/+;slboGal4, SEADR/+*

Migrating clusters

$p<0.0001$

Front of the lead cell (f)

Side of the lead cell (s)

f RTK RNAi
Localization index
(lead cell)

***

Front/Cytoplasm (f/c)

Control   PVR+EGFR

g Localization index
(lead cell)

***
***

Front/Cytoplasm (f/c)

Control   Ras(TRiP)   Ras(GD)

h Polarization index
(lead cell)

***
***

Front/Side (f/s)

Control   Ras(TRiP)   Ras(GD)

Figure 2

a   Wild Type :*slboGAL4, slbo-SEDAR, 2xslbo-turboRFP/+*

<<<<RFP   GFP>>>>

b   Early Migrating clusters

c   Late Migrating clusters

d   Early Migrating clusters
p<0.0001
n=441

e   Late Migrating clusters
p<0.0001
n=363
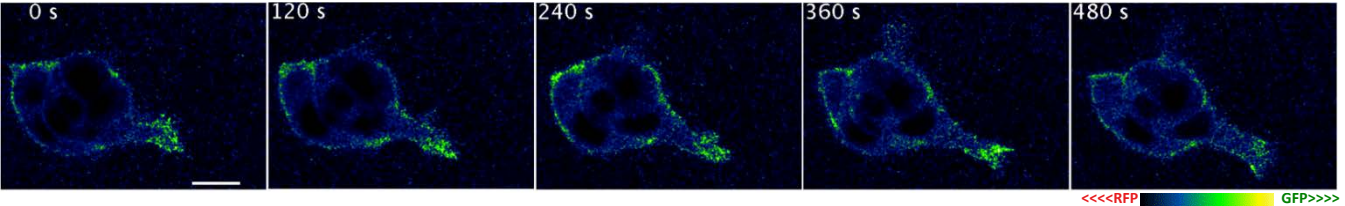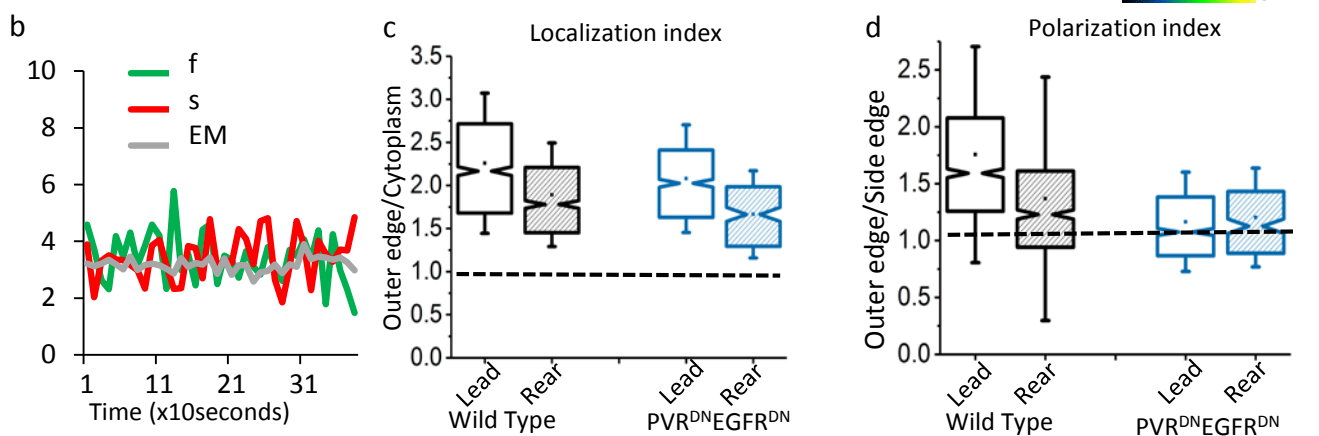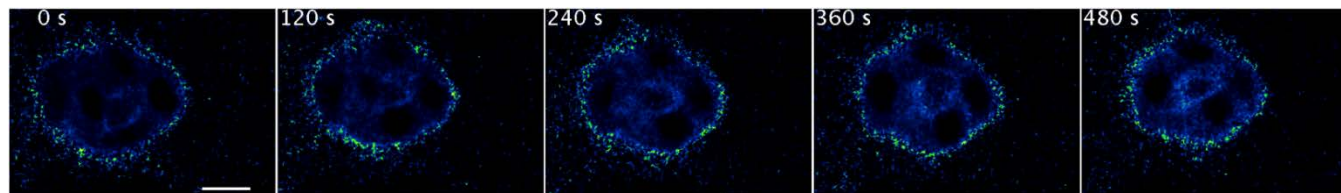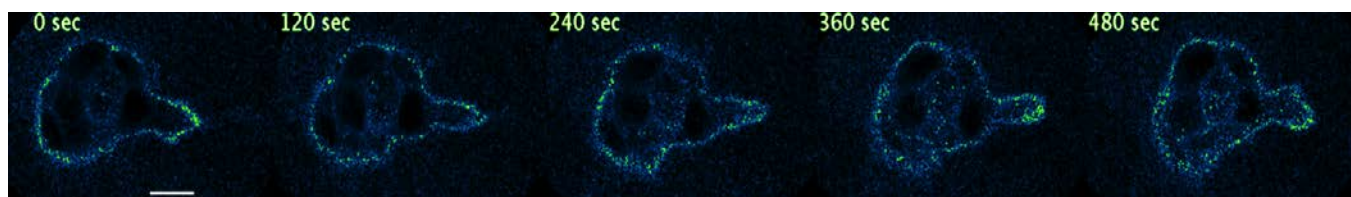
f   Localization index

g   Polarization index
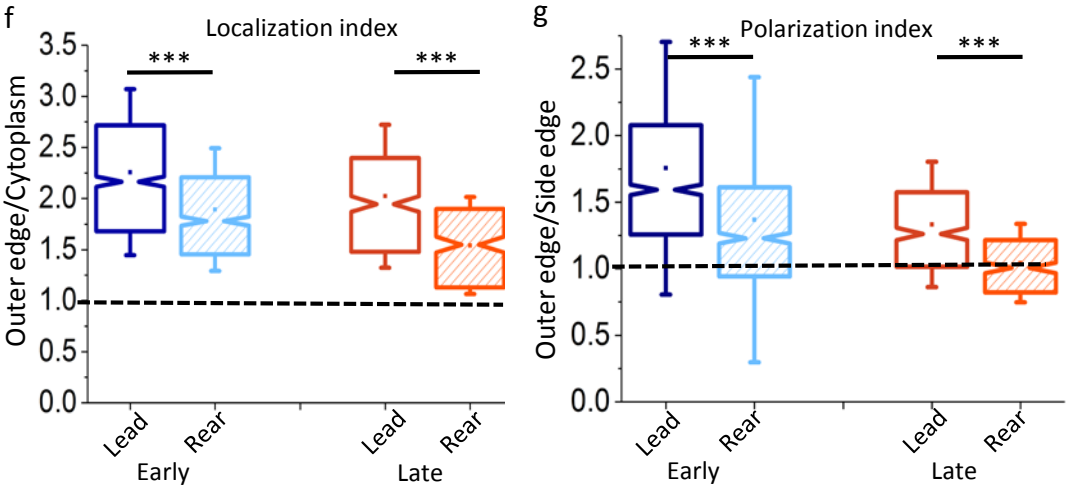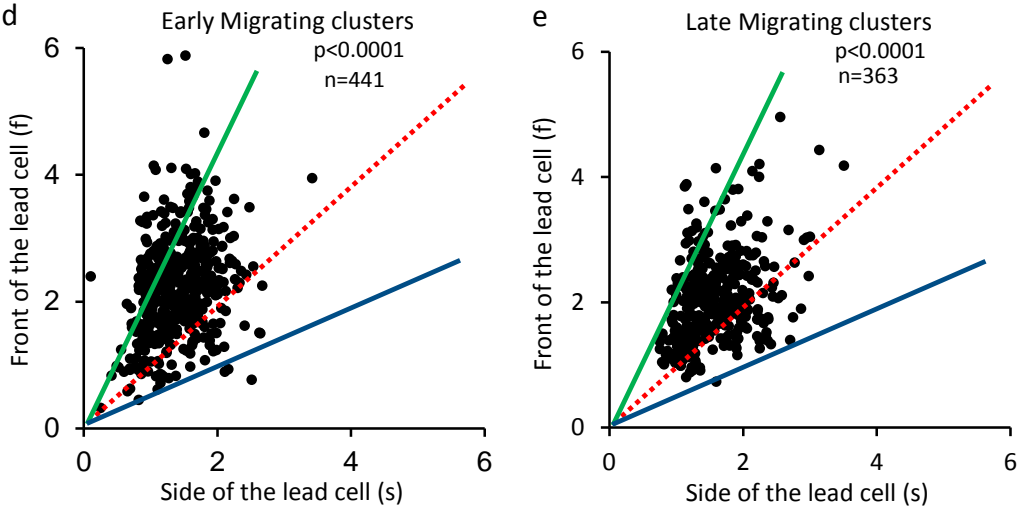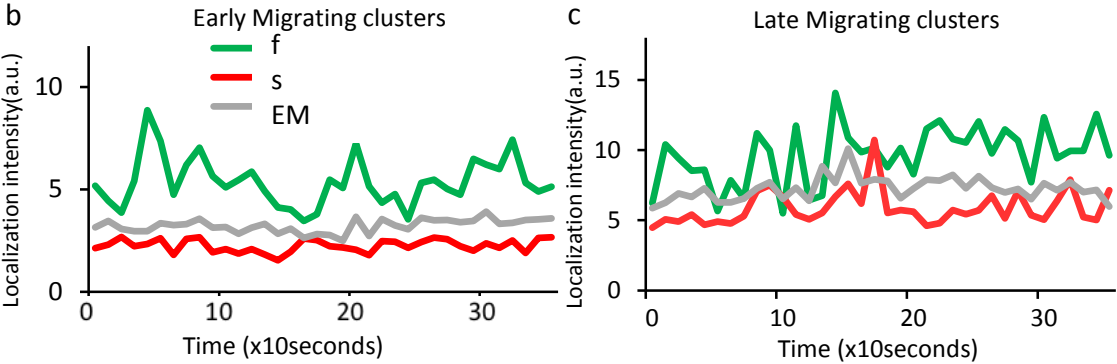
Figure 3

a PVR^{DN}EGFR^{DN}: *UAS-EGFR^{DN}, UAS-PVR^{DN}/+;slboGAL4, slbo-SEDAR, 2xslbo-turboRFP /+*

e PVR: *UAS-PVR/+;slboGal4, slbo-SEDAR, 2xslbo-turboRFP /+*

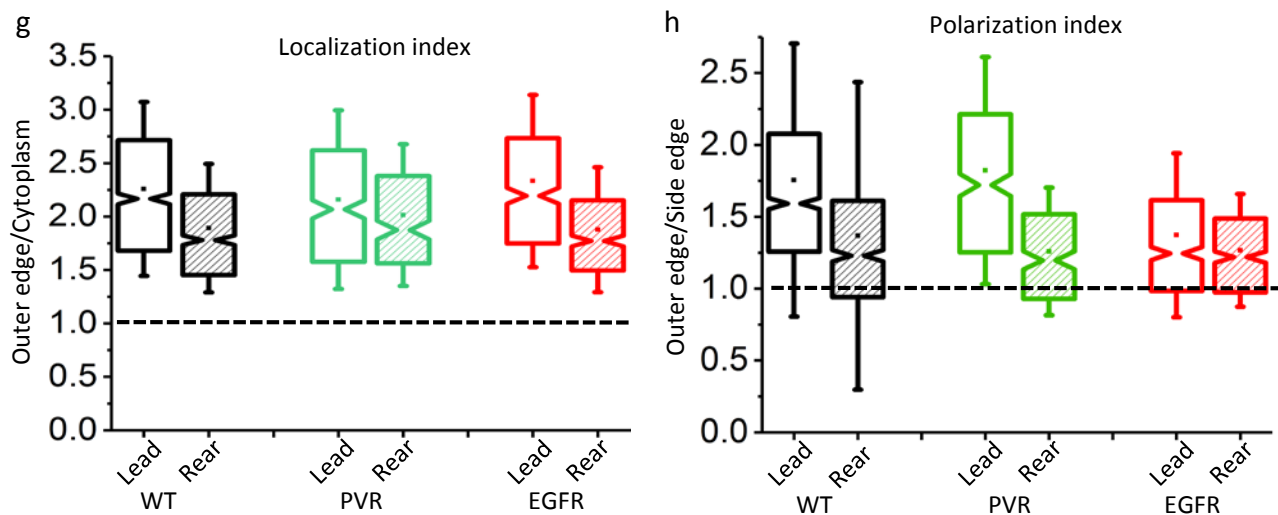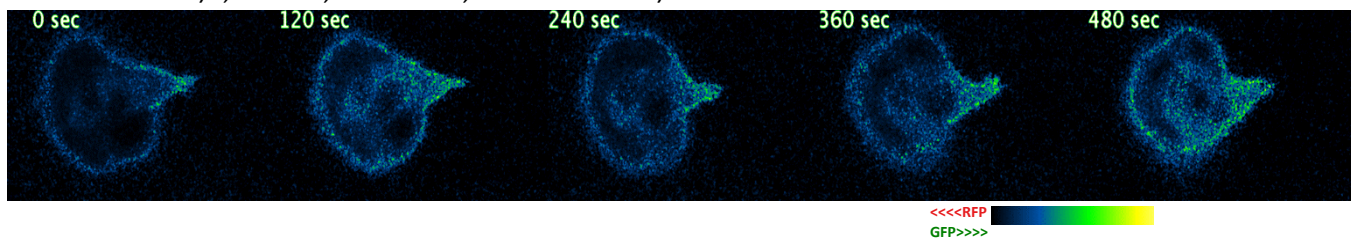f EGFR: *UAS-EGFR/+;slboGal4, albo-SEDAR, 2xslbo-turboRFP /+*

Figure 4

a   Stage 13 epidermis during dorsal closure

hsSEDAR/+

b   Ovariole

hsSEDAR/+

Stage 4   Stage 6   Stage 8

Stage2

Zoom in Stage 7

c

Receptor   SEDAR   Actin

PVR

EGFR

PVR :*UAS-PVR/+;slboGal4, hs-SEDAR/+* & EGFR :*UAS-EGFR/+;slboGal4, hs-SEDAR/+*